*Revised Manuscript
Click here to view linked References

Remediation of ^{137}Cs Contaminated Concrete Using Electrokinetic Phenomena and Ionic Salt Washes in Nuclear Energy Contexts.

Andrew J. Parker[1], Malcolm J. Joyce[2], Colin Boxall[2]

[1]*Department of Science, Natural Resources and Outdoor Studies, University of Cumbria, Bowerham Road, LA1 3JD, UK*

[2]*Department of Engineering, Lancaster University, Bailrigg, LA1 4YR, UK*

Abstract

This work describes the first known the use of electrokinetic treatments and ionic salt washes to remediate concrete contaminated with ^{137}Cs. A series of experiments were performed on concrete samples, contaminated with K^+ and ^{137}Cs, using a bespoke migration cell and an applied electric field (60 V potential gradient and current limit of 35 mA). Additionally, two samples were treated with an ionic salt wash (≤ 400 mol m^{-3} of KCl) alongside the electrokinetic treatment. The results show that the combined treatment produces removal efficiencies three times higher (>60%) than the electrokinetic treatment alone and that the decontamination efficiency appears to be proportional to the initial degree of contamination. Furthermore, the decontamination efficiencies are equivalent to previous electrokinetic studies that utilised hazardous chemical enhancement agents demonstrating the potential of the technique for use on nuclear licensed site. The results highlight the relationship between the initial contamination concentration within the concrete and achievable removal efficiency of electrokinetic treatment and other treatments. This information would be useful when selecting the most appropriate decontamination techniques for particular contamination scenarios.

Keywords

137-Caesium; Electrokinetic Decontamination; Ionic Salt Washes; Concrete Remediation; Nuclear Decommissioning

1. Introduction

In the United Kingdom, the activities involved in the nuclear fuel cycle have generated a large national inventory of hazardous radioactive material, specifically at legacy facilities such as the Sellafield site, including a large volume of contaminated buildings and surfaces [1]. Specifically, the UK Nuclear Decommissioning Authority estimates there to be >3,000,000m^3 of radioactively-contaminated concrete at sites it has responsibility for decommissioning [2]. Consequently, the decontamination and remediation of these sites, and subsequent disposal of contaminated material, is one of the largest engineering challenges facing the UK nuclear industry.

Due to limited space in waste repositories, the UK strategy for managing radioactive wastes has placed an emphasis on adopting the 'Waste Hierarchy' [3]. As such, increased focus has been on removing contamination from building materials prior to demolition with the aim of minimising the volumes of radioactive waste sent for disposal.

Most decontamination techniques adopted in the UK fall into two principal types, mechanical and chemical. Both are effective but have significant drawbacks in the secondary wastes they produce and the hazardous nature of the techniques [4–6]. Accordingly, there is an ongoing requirement to discover new treatments which combine the effectiveness of existing decontamination treatments with reduced operational hazard. One such technique is electrokinetic remediation: the use of an applied electric field to induce the migration of charged materials in a saturated porous medium [7]. The technique has been utilised for the treatment of land, soils, gravels contaminated with halogens [8], hydrocarbons [9,10], heavy metals [11–15], pesticides [16], and radionuclides [17–20], with ongoing studies to scale-up the technique [21]. However, research into its potential as a concrete decontamination technique has been limited.

2. *Electrokinetic Radioactive Concrete Remediation Techniques*

The application of electrokinetic concrete remediation can be divided into three categories based on the physical form of the concrete and its arrangement relative to the electrodes and electrolyte. The categories are: the *ex situ* treatment of crushed concrete, the *ex situ* treatment of intact monoliths; the remediation of intact concrete surfaces *in situ*.

2.1. Ex Situ Crushed Materials

Crushing concretes offers two advantages over *in situ* electrokinetic remediation of concrete monoliths: Firstly, crushing concrete increases the available surface area for decontamination which reduces the time taken to achieve acceptable levels of radionuclide extraction, especially for radionuclides that have migrated deep into a concrete matrix. Secondly, using dedicated facilities provides for greater process control, allowing a wider range of reagents and washing techniques not permissible under on-site regulations. The major disadvantage is that demolishing contaminated buildings for transport to a facility can generate large amounts of radioactive particulate, creating a respiratory hazard [22].

Kim et al. studied the effects of electrokinetic treatment on crushed concrete (0.6-1.2mm particle size) washed with HCl prior to remediation [23].Their results show that for unwashed concrete, a 15 day treatment removed ~60% of Cs^{+} and negligible levels of Co^{2+} (~0.9%). Washing the crushed concrete with 3 mol dm^{-3} HCl for 4 hours before the electrokinetic treatment increased removal efficiencies to a maximum of 99.7% for Co^{2+} and 99.6% for Cs^{+}. Additionally, a second work by Kim et al. studied pre-treatment washing with H_2SO_4, which increased removal efficiencies to 99.6% for Co^{2+} and 99.3% for Cs^{+}. Additionally, crushed concretes (0.6-1.2mm particle size), containing ^{60}Co and ^{137}Cs, were also treated [24]. Entrained ^{60}Co (420Bq kg^{-1}), was removed by ~98.45% and ^{137}Cs (560Bq kg^{-1}) by ~87.18% [24].The increase in removal efficiency, compared to the unwashed trials, was attributed to the acid wash lowering the concrete pH to ~3.7. The reduction in pH causes $CaCO_3$ in the concrete to decompose to CO_2, allowing bound radionuclides to become available for transport. The lowering of concrete pH also prevents Co^{2+} from forming $Co(OH)_2$, which occurs above pH 6, hence the rise in Co^{2+} removal efficiency between unwashed and washed concretes.

Similarly, Yurchenko et al. carried out electrokinetic decontamination of concrete rubble contaminated with uranium, with individual concrete pieces being ≤ 3kg [25]. In total, 93kg of rubble was placed inside a migration cell similar to the one used by Kim et al. [25]. Their results show that an 800 hour electrokinetic treatment accelerated uranium removal by a factor of 70-140 compared to a static regime, with a maximum removal efficiency of 95%.

The results of both studies by Kim et al. and by Yurchenko et al. on the application of electrokinetic regimes on crushed concrete show that the dominant transport phenomenon occurring is electromigration, accounting for ~94% of total ion transport [23–25].

2.2. Ex Situ Treatment of Monoliths

The treatment of concrete monoliths is comparable to the remediation of crushed concretes, with the physical form of the concrete being the only difference. Monoliths require less processing prior to decontamination but the decrease in surface area compared to crushed concretes typically reduces the decontamination efficiency.

Popov et al. observed the 3-fold increase in Cs^+ decontamination that 9-hour electrokinetic application had on Cs^+ removal from the surface of a monolithic concrete sample compared to a static regime (23.2% no voltage, 61.5% electrokinetic) [26].Their work also showed EDTA acted as a superior electrolyte for removing Cs^+ compared to distilled water, (0.067mmol l^{-1} of Cs^+ removed for EDTA and 0.048mmol l^{-1} for distilled water). A second study by Popov et al. described the decontamination of a 128cm^{-3} concrete monolith, reporting removal efficiencies of 30.8% ^{137}Cs and 40.4% ^{60}Co, respectfully, after 3600 minute application [27]. As reported in the studies above, 90% of Cs^+ ions were transported toward the cathode via electromigration [27].

2.3. In Situ Decontamination

The electrokinetic decontamination of concrete surfaces is the most direct example of *in situ* concrete decontamination. The technique utilises comparatively large electrode setups (~1.7 m^2) to cover contaminated concrete surfaces. Counter electrodes are either placed into the concrete, through drilling, or structural concrete reinforcement bars are used.

DePaoli studied the electrokinetic transport of Cs^+, Sr^{2+}, Co^{2+}, and U^{3+} through a 9.5mm concrete disk, mimicking the contamination and subsequent decontamination of concrete surfaces [28]. The authors found only Cs^+ was readily removable (with over 95% of Cs^+ transported through and removed from the concrete sample): 63% of Co^{2+} precipitated onto the exposed surface and 73% of the Sr^{2+} used was retained within the sample.

Castellote et al. demonstrated a range of *in situ* electrokientic treatments for samples and surfaces artificially contaminated with Cs^+, Co^{2+}, Sr^{2+} and Fe^{3+} [29]. The first two experiments consisted of casting concrete cylinders and contaminating them through the addition of contaminates during mixing or contaminating the exposed cathode-facing surfaces. The application of varying electrokinetic treatments on these samples led to a reduction in Cs^+ content in the samples by 25-

40% from experiments with Cs^+ in the casting solution and 75-95% from Cs^+ surface decontamination, with the higher removal efficiencies found in the samples with greater initial contamination.

A third experiment by Castellote et al. adopted a honeycomb electrode arrangement placed over the sample using tap water as the electrolyte [29].The extraction of Cs^+ from the four tested areas averaged ~83 %, and removed contaminates from a depth of 10mm. Further analysis of the slab showed that even Cs^+ initially present on the lateral sections of the slab had been removed. Despite a shallow depth of contamination, no extraction was detected for Co^{2+}, Sr^{2+} and Fe^{3+}.

Frizon et al. conducted an experimental study largely similar to one of those carried out by Castellote et al., specifically electrokinetically decontaminating a concrete cylinders contaminated with non-active Cs^+ [30]. Their results are consistent with those of Castellote et al., that higher initial contaminations lead to higher removal efficiencies, specifically ~95% and ~81% for samples contaminated with 0.309 and 3.84 x 10^{-3}mmol cm^{-3}, respectively.

The first example of *in situ* concrete decontamination on a field test was conducted by Lomasney et al. [31]. Their work focused on the removal of thorium from concrete at the US Department of Energy site using a bespoke Surface Electrokinetic Extraction Pad (SEEC). They recorded removal efficiencies ~82% for ^{252}Th using nitric acid as the electrolyte. This work was built upon by Popov et al. further demonstrating surface decontamination using SEEC in the effective removal of ^{252}Th, $^{235}/^{238}U$, ^{60}Co, ^{90}Sr and ^{137}Cs from a 1.8m^2 surface using citric acid in the electrolyte [31]. Their results demonstrate 100% removal of uranium, thorium and cobalt after 500 minutes of application. Sr^{2+} and Cs^+ were again slower to be removed as they possess a lower complexing forming ability, with the citric acid electrolyte.

Table 1. Experimental removal efficiency, decontamination factor, and initial concentration for literature studies closely resembling the design of this study (above dashed line) and studies with different experimental geometry or electrolyte enhancement is used (below dashed line).

Study	Contaminant	Thickness (mm)	Approximate Contamination (mmol cm^{-3})	Removal Efficiency	DF
DePaoli et al. (1995)	Cs^+	9.5	1.8×10^{-3}	95%	20
Castellote et al. (2002) 1	Cs^+	30	1.4×10^{-3}	95%	20
Castellote et al. (2002) 2	Cs^+	75	1.51×10^{-7}	40%	1.67
Frizon et al. (2005) 1	Cs^+	18	3.84×10^{-3}	81%	5
Frizon et al. (2005) 2	Cs^+	18	0.309	95%	23

Castellote et al. (2002) 3	Cs^+	-	5.11×10^{-3}	90%	10
Popov et al. (2008) 1	Cs^+	-	3.45×10^{-16}	31%	1
Popov et al. (2008) 2	$^{137}Cs^+$	-	-	85%	7
Kim et al. (2009) 1	Cs^+	-	4.61×10^{-3}	55%	2.2
Kim et al. (2009) 2	Cs^+	-	4.63×10^{-3}	99.60%	250
Kim et al. (2010) 1	$^{137}Cs^+$	-	1.16×10^{-11}	52%	2
Kim et al. (2010) 2	$^{137}Cs^+$	-	1.16×10^{-11}	99.30%	143
Castellote et al. (2011)	Cs^+	10	-	90%	10

2.4. Removal Efficiency Enhancement

Electrokinetic remediation can only extract contaminants that are mobile, as demonstrated in the above studies where Cs^+ was the only contaminate extracted to a significant degree without the addition of any reagents, since Cs^+ is soluble over a wide range of pH. Other isotopes (^{60}Co, ^{90}Sr, ^{238}U etc.) precipitate out in the high pH environments of concrete pore solutions inhibiting their removal. Additionally, the adsorptive properties of concrete further prohibit ionic migration, particularly for some of the radionuclides of interest [32,33]. Because of these factors, electrokinetic concrete decontamination has adopted a range of electrolyte manipulation and sample pre-treatment techniques. These techniques are designed to transform contamination into a form that is readily transportable. Dissolving the concrete and contaminates in strong acid (HCl, H_2SO_4), or forming complexants and chelates (EDTA, citric acid, nitric acid, acetic acid) have all been shown to be effective [24,27]. However, facilities used in the nuclear fuel cycle maintain strict regulations on the use of hazardous and toxic substances. This makes the use of EDTA and strong acids in electrokinetic field trials problematic. Of the reagents used, only citric acid meets conventional safety standards for use on nuclear sites.

2.5. Reducing the Hazard

Most studies outlined above adopt hazardous reagents to enhance the removal efficiency of the electrokinetic technique. To increase the possibilities of operational deployment, enhancement techniques must be sort that maintain the effectiveness of the electrokinetic treatment but negate the chemical hazard. One possible approach outlined by Kaminski *et al.* are ionic washes, the use of inert ionic salts (e.g. NaCl, KCl, NH_4) to ion exchange with contaminates [34]. Kaminski *et al.* note that although the ionic washes are effective at ion exchanging with contaminates, once exchanged, these contaminates can migrate deeper into a surface. By incorporating electrokinetic techniques with ionic washes it could be possible to control the process of ion exchange and allow the contamination to be safely removed from the concrete or building materials.

Therefore, the aim of this study is to demonstrate the use of electrokinetic techniques in combination with ionic washes to remove ^{137}Cs from concrete, establishing the effectiveness of electrokinetic treatments without the need to use hazardous chemicals. This would allow the treatment, which has been shown to be one of the most cost effective decontamination techniques [35], to be more widely adopted on nuclear licensed sites in the effort to decontaminate and dispose of the vast amount of radioactive contaminated concrete materials.

3. Materials and Method

3.1. Concrete

The concrete samples used throughout this work were mixed with a 3:2:1 ratio (pebble aggregate, standard siliceous sand, and Ordinary Portland Cement respectively) based on European Standard EN 196-1, with a water to cement mass ration of 0: 5. The concrete was poured into cylindrical polypropylene moulds, 150 mm long with an inner diameter of 105 mm, and left to cure for 28 days. At the end of the curing period the cylinders were cut into smaller thickness sections (20, 25, 35, 65 mm).

Following this, concrete samples were artificially contaminated using baths of KCl or ^{137}Cs, utilising cationic diffusion as the mechanism for contamination. To achieve equilibrium, samples were sealed in the contamination baths for 50 days and shaken periodically, concentrations of the contamination solutions are shown in Table 2. After this period the samples were rinsed in deionised water and dried at 50°C for seven days to remove moisture. The samples were then analysed radiometrically to discern the relative contamination, showing a maximum adsorbed contamination of 0.521 and 3.551 x 10^{-9} mmol cm^{-3} for K^+ and ^{137}Cs respectively; all details of the initial activities and adsorbed masses of contamination are detailed in Table 2.

Table 2. Composition of the contamination baths and the initial mass of contamination adsorbed onto the concrete samples, for both the K^+ and ^{137}Cs samples (all ^{137}Cs samples were 25 mm thick).

Sample No.	Contaminate	Thickness (mm)	Concentration of Bath (mmol cm^{-3})	Activity Sorbed (kBq)	Mass Sorbed (mmol cm^{-3})
1	K^+	20	3	0.121 (±0.009)	0.521

2		20	3	0.105 (±0.007)	0.454
3		35	3	0.206 (±0.014)	0.508
4		65	3	0.157 (±0.010)	0.208
			Activity of Bath ($kBq\ ml^{-1}$)		
5	$^{137}Cs^{+}$	25	0.889	328.25 (±0.56)	3.551×10^{-9}
6		25	0.604	268.61 (±0.40)	2.906×10^{-9}
7		25	0.089	39.68 (±0.08)	4.293×10^{-10}
8		25	0.042	22.61 (±0.05)	2.446×10^{-10}

3.2. Experimental Phantom and Detector

The electrokinetic experiments were carried out using a radioanalytical phantom, Figure 1. The experimental setup was similar to the one described in previous works [36,37], as such only a concise description is given here. Concrete samples were sealed into a polypropylene pipe connecting two electrolyte compartments: each of volume 1.04 litres. The external DC necessary for the generation of electrokinetic transport was provided by an EL302T power supply (Thrulby Thandar Instruments), set to an applied voltage of 60V. The power supply was connected to a mild-steel reinforcement bar cathode, and a platinised titanium mesh anode. The anode and cathode were mounted 50mm from the surface of the concrete samples within the respective compartments. Two additional platinum electrodes were placed at the anodic and cathodic-facing surfaces of the samples to measure the potential difference across their length. To prevent electrolyte heating, and unwanted electroosmotic flow, the current was limited to 35mA. The electrolyte contained a 100mol m^{-3} NaOH solution to match the alkaline cementitious pore solutions and the conditions found in nuclear fuel storage ponds.

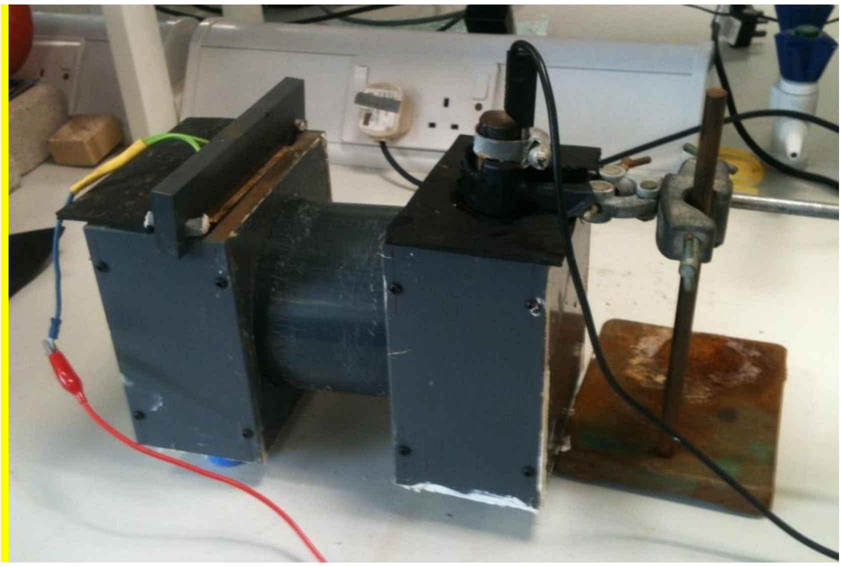

Figure 1. Radioanalytical phantom used in this work, the anode compartment (left) contains platinised titanium mesh, the cathode compartment (right) contains mild steel cathode.

The decontamination of concrete samples was assessed radiometrically: ^{137}Cs decontamination using a CsI(Tl) scintillator; K^+ contaminated samples using a bespoke NaI(Tl) well-type scintillation counter [38]. The radioactivty of the samples contaminated with ^{137}Cs allowed for *in situ* counting of the cathloyte compartment, see Figure 2. Where ^{40}K was the isotopic tracer 40ml aliquots of the anolyte and chatholyte solutions were removed from the phantom and counted for 4 hours before being replaced in their respective electrode compartment. Similarly, the activity of each concrete sample was measured before and after decontamination.

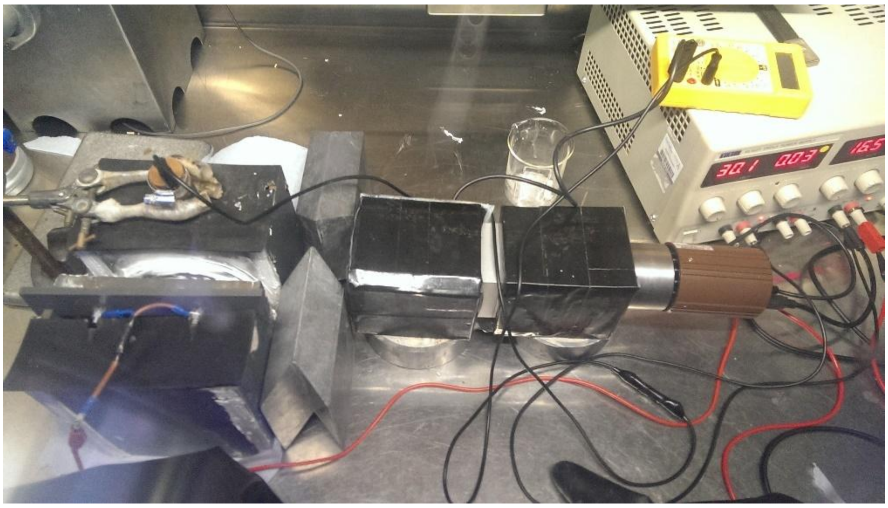

Figure 2. Photograph of the in situ CsI(Tl) detector setup used to monitor the decontamination of ^{137}Cs , where the detector is surrounded with a lead collimator sheath with the circular aperture cut into the centre.

4. Results and Discussion

The experimental decontamination protocol used was the same for both the samples contaminated with K^+ and $^{137}Cs^+$ respectfully (with the exception of using an ionic wash for two of the ^{137}Cs samples). The protocol was run until a substantial decrease in the rate of contamination entering the catholyte was observed. Following this the samples were removed, washed, oven dried, and analysed radiometrically as before.

4.1. Potassium Decontamination

It can be seen from Figure 3 that the majority of K^+ was removed within the first 300 hours, after which the count increases until reaching a plateau after approximately 700 hours of treatment for Sample 2. At the conclusion of the experiment the K^+ concentration in the cathode compartment was 74mol m^{-3}, corresponding to 2.9g or 95.5 ± 5% of the initial potassium contamination removed from Sample 2.

Similar catholyte count profiles were observed for the 35 and 65mm samples when exposed to the electrokinetic treatment, recording removal efficiencies of 70.1 ± 3% and 90.1 ± 6% respectively. This trend is consistent with the results for the ^{137}Cs decontamination, see Figure 4, and the results of Castellote *et al.* (2002) who observed a potential trend where the most of the contamination is released in the early stages of the treatment [29]. Also consistent with Castellote *et al.* (2002), negligible amounts of K^+ were detected in the anolyte, evidence that the primary transport mechanism during the experiment was electromigration.

Also shown in Figure 3, is the fraction of K^+ contamination remaining at the conclusion of the treatment. In all samples where the electric field was applied there was a pronounced decrease in the K^+ content remaining in the samples at the conclusion of the experiments. In contrast, no decrease was detected in Sample 1 which did not undergo electrokinetic treatment. These results show that the application of the electric field significantly promotes the transport of ions from the samples.

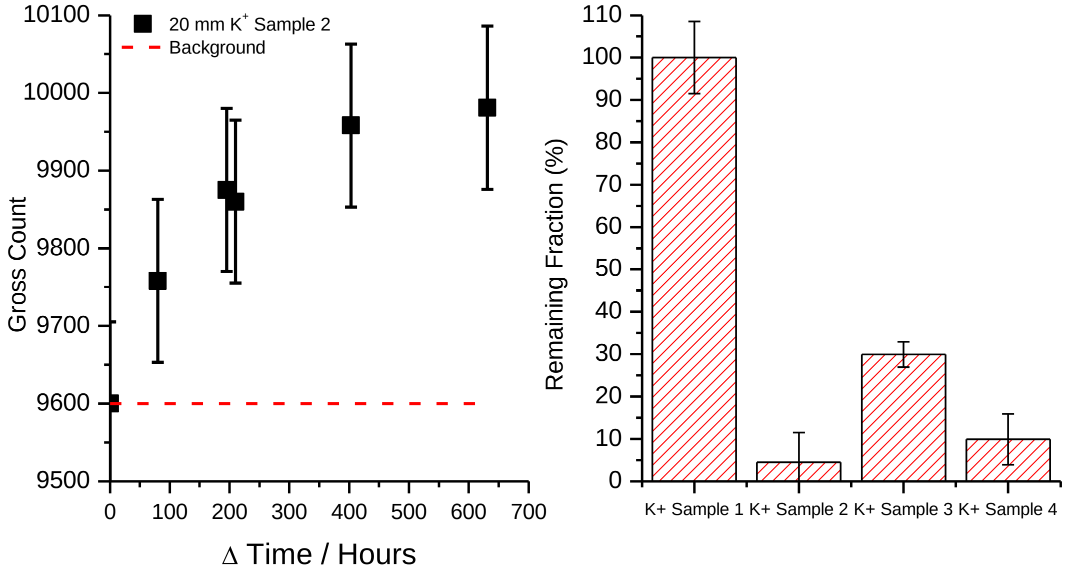

Figure 3. Variation with time in K^+ concentration (as indicated by the gross radioactive count) in the cathoylte solution as a result of the application of an external electric field (60V, 35mA) over concrete sample 2 (left). Fraction of K^+ remaining in Samples 1-4 at the conclusion of decontamination treatment (right). Errors bars indicate 3 σ.

4.2. Caesium Decontamination

As in the potassium decontamination experiments, once the electric field is applied a rapid change in contamination removal was observed. During this change the count rate detected in the catholyte followed a near exponential increase with time, reaching a near-linear increase after ~130 hours. The observed increase in catholytic gross count with time is consistent between the two samples studied, Sample 5 and 7, as shown in Figure 4. Though it can be seen that for both samples the catholyte count had not reach a plateau, indicating ^{137}Cs was still being removed when the experiments were terminated, the post-treatment assessment shows that only ~20% was removed from each sample. This is significantly lower than the removal efficiency recorded for the K^+, where the removal efficiency ranged from 70-95.5%

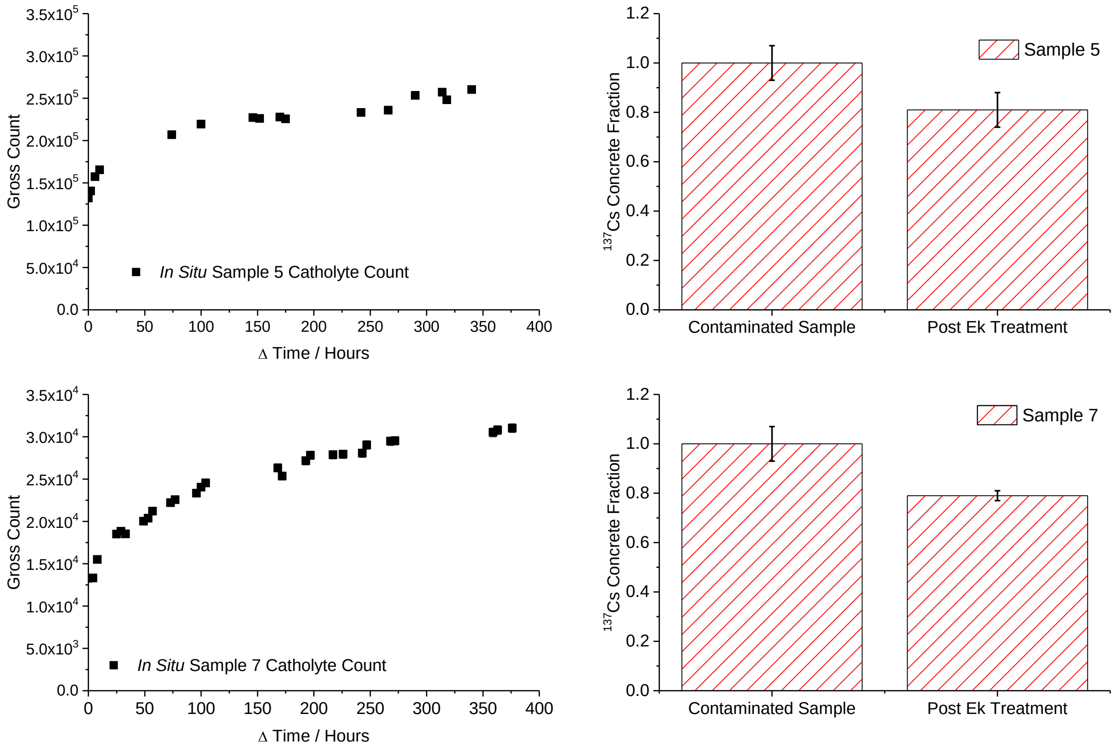

Figure 4. Variation with time in $^{137}Cs^+$ catholyte gross count during application of an external electric field (60V, 35mA) over concrete Samples 5 and 7, 328 and 40kBq respectively (left). Fraction of $^{137}Cs^+$ remaining in Samples 5 and 7 after 360 hours of decontamination treatment (right). Errors bars indicate 3 σ.

Adopting the ionic salt wash to the electrokinetic treatment of ^{137}Cs contaminated concrete (Samples 6 and 8), shows a difference compared to that of the non-wash ^{137}Cs samples (Samples 5 and 7). As can be seen in Figure 5, for both experiments the addition of KCl to the anolyte solution (400 and 135mol m^{-3} for Samples 6 and 8 respectively) produced a upsurge in the ^{137}Cs removed from the concrete, where the red vertical line corresponds to the point at which the KCl was added. Prior to the KCl addition it can be seen in both experiments that the rate of Cs is relatively modest and broadly similar to the extraction rates seen in Sample 5 and 7. Following introduction, the rate of removal dramatically increases then slows, plateauing after ~450 hours of treatment in both Sample 6 and 8. There is an argument to say that the rate of ^{137}Cs removal decreased because the majority of the K^+ ionic wash had been used, however a significant proportion of K^+ was still detected in the anolyte. As can also be seen from Figure 5, the effect on the final removal efficiencies was as significant, increasing to 40 and 60% respectively for the two samples.

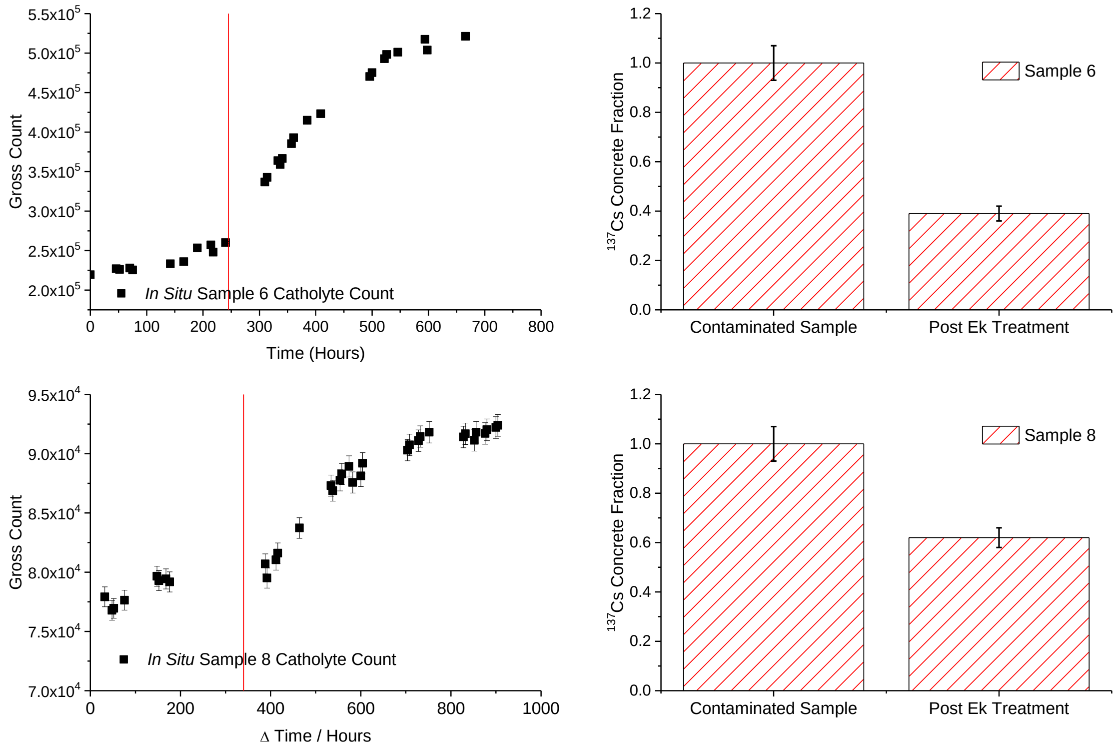

Figure 5. (Left) Change in the in situ catholyte gross count over time, (Right) change in activity of ^{137}Cs Samples 6 and 8 (269 and 23kBq respectively) after 900 hours of electrokinetic treatment. The vertical red line indicates the point of KCl addition, 400 and 135 mol m^{-3} for Samples 6 and 8 respectively. Errors bars indicate 3 σ.

Table 3. Complete results from the electrokinetic decontamination of concrete samples contaminated with K+ and $^{137}Cs^{+}$ carried out in this study.

Sample No.	Contaminant	Thickness (mm)	Initial Contamination (mmol cm^{-3})	Removal Efficiency	DF	Ionic Wash (mol m^{-3})
1	K^+	20	0.521	0.8 ± 5%	1	-
2		20	0.454	95 ± 7%	22.22	-
3		35	0.508	70 ± 3%	3.44	-
4		65	0.208	90 ± 6%	10.12	-
5	$^{137}Cs^{+}$	25	3.551×10^{-9}	19 ± 0.13%	1.24	-
6		25	2.906×10^{-9}	*60± 0.13%	2.5	400
7		25	4.293×10^{-10}	20 ± 0.47%	1.26	-
8		25	2.446×10^{-10}	*37 ± 0.59%	1.58	135

The results from the potassium and caesium decontamination are shown in Table 3, along with the initial level of contamination. The most striking observation from these results is the difference in removal efficiency between the potassium contaminated samples and those with ^{137}Cs, with a mean removal efficiency approximately 50% higher for potassium over caesium. Given that the methods employed to contaminate and decontaminate were similar, the reason for this disparity is not immediately apparent.

An explanation is that the significant difference between the contamination levels, and therefore number of ions, present in the samples affect the removal efficiency. This conclusion has previously been alluded to in other studies after similar findings of higher ionic loading and higher removal efficiency were observed to concrete samples contaminated with two different masses [29,30]. Based on the activity, the ^{137}Cs was in the range of 0.53-7.68 x 10^{-10} moles, compared to between 0.08 and 0.15 moles of potassium. The large difference in the ion loading between the two sample batches may have a significant effect on the decontamination efficiency observed in the experiment due to the interaction between the contaminating ions and the concrete matrix.

A variation in removal efficiency with loading would be expected from materials that present a range of adsorption sites within the concrete matrix with differing adsorption strengths. At low ionic loading the strongly adsorbing sites would be occupied preferentially, making removal difficult, and at high ionic loading both strong and weaker adsorbing sites will be occupied, resulting in a higher removal efficiencies. Sites of differing adsorption strength would be expected of chemically composite or inhomogeneous materials, such as concrete or cement [32,33]. In this instance, therefore, the tiny volume of ^{137}Cs in the samples is likely adsorbed onto strongly adsorbing sites on the aluminosilicate mineral structure of the concrete.

The capacity of concrete to retain cations varies depending on a range of physicochemical and compositional factors. In this instance, it is likely that the adsorption capacity of the concrete samples is greater than the mass of ^{137}Cs used to contaminate the samples based on a conservative adsorption capacity estimate of 1 x 10^{-4}mol kg^{-1} [32,33]. Conversely, there is a significantly larger mass of K^+ in the potassium samples, ~0.1 mole, than there is likely the capacity of adsorption sites. As a result, K^+ will saturate the adsorption sites leaving the vast majority of K^+ in the pore solution.

When the concrete samples are removed, washed, and dried at the conclusion of the contamination phase a fraction of the K^+ in the pore solution will precipitate as the pore water evaporates. Hence, when the sample is placed back in the radiological phantom for decontamination with DDW the precipitated K^+ re-dissolves in the new pore solution. The K^+ in the pore volume is therefore available for electrokinetic transport on application of the external electric field and easily removed. In contrast, the concentration of caesium in the experiments was far lower than that of potassium, consequently the lower mass of Cs^+ is likely adsorbed onto the concrete matrix, occupying the strongly adsorbing sites first. Strongly adsorbed Cs^+ will be more resistant to electrokinetic removal from the matrix, as appears to be the case, in addition to the cementitious material having a greater affinity for Cs^+ over K^+.

This hypothesis is reinforced by the results from the Cs^+ decontamination studies incorporating the ionic salt wash. The ionic salt provides ions to displace the adsorbed Cs^+ via uni-univalent ion exchange, shown in Eq. 1. [39], which then electromigrate out of the concrete into the catholyte. Hence, the observed increased rate of Cs^+ entering the catholyte in Figure 5 and the final decontamination efficiencies for these two trials, Table 3.

$$\overset{\text{CONCRETE}}{M^-Cs^+} + \overset{\text{SOLUTION}}{K^+} \leftrightarrow \overset{\text{CONCRETE}}{M^-K^+} + \overset{\text{SOLUTION}}{Cs^+} \qquad \text{Eq. 1}$$

The lower removal efficiency for Sample 8 compared to Sample 6 is further evidence of the loading effects. The two samples had an order of magnitude difference in initial contamination, given these loading effects, one may expect a lower mean removal efficiency for samples of lower contamination as the strongly adsorbing sites are the most difficult to access, even with highly concentrated ionic washes.

4.3. Comparison with Other Studies

It is clear from Most studies outlined above adopt hazardous reagents to enhance the removal efficiency of the electrokinetic technique. To increase the possibilities of operational deployment, enhancement techniques must be sort that maintain the effectiveness of the electrokinetic treatment but negate the chemical hazard. One possible approach outlined by Kaminski *et al.* are ionic washes, the use of inert ionic salts (e.g. NaCl, KCl, NH_4) to ion exchange with contaminates [34]. Kaminski *et al.* note that although the ionic washes are effective at ion exchanging with contaminates, once exchanged, these contaminates can migrate deeper into a surface. By incorporating electrokinetic techniques with ionic washes it could be possible to control the process of ion exchange and allow the contamination to be safely removed from the concrete or building materials.

that a range of removal efficiencies have been recorded that are broadly consistent with the results in this study, however full comparison is difficult for the reasons described in Section 2.5. Castellote et al. (2002) refer to this issue and proposed evaluating decontamination efficiencies against the amount of charged passed when electromigration is the dominant transport mechanism [29]. Even this approach is flawed as the inclusion of NaOH to manage electrolyte pH is common, as well as the presence of competing ions in the concrete and electrolytes all provide additional charge carriers which could distort the comparison. One base-line for comparison is the amount of contamination present in the samples prior to treatment.

With the exception of the studies by Kim et al., which studied crushed concrete, the other examples identified in Section 2 broadly follow the pattern outlined above: higher initial contamination leads to higher removal efficiencies, as seen in Figure 6. The studies largely fit into two distinct groups, with a cluster of highly contaminated samples (> 1 x 10^{-3}mmol cm^{-3}) and a grouping of lower contamination (<1 x 10^{-6}mmol cm^{-3}). The separation of groups supports the hypothesis that a low-level of contamination is bound to the strongly adsorbing sites which fill rapidly at higher concentrations, leaving the majority of contamination precipitated into the concrete pore volume when dried. This relationship is evident between the K^+ and ^{137}Cs contaminated samples in this work and further supports the connection between the degree of contamination within a concrete and the adsorptive capacity of that concrete. This implies a threshold above which the contamination can be readily removed by electrokinetic treatment without the aid of salt washes or other enhancement techniques.

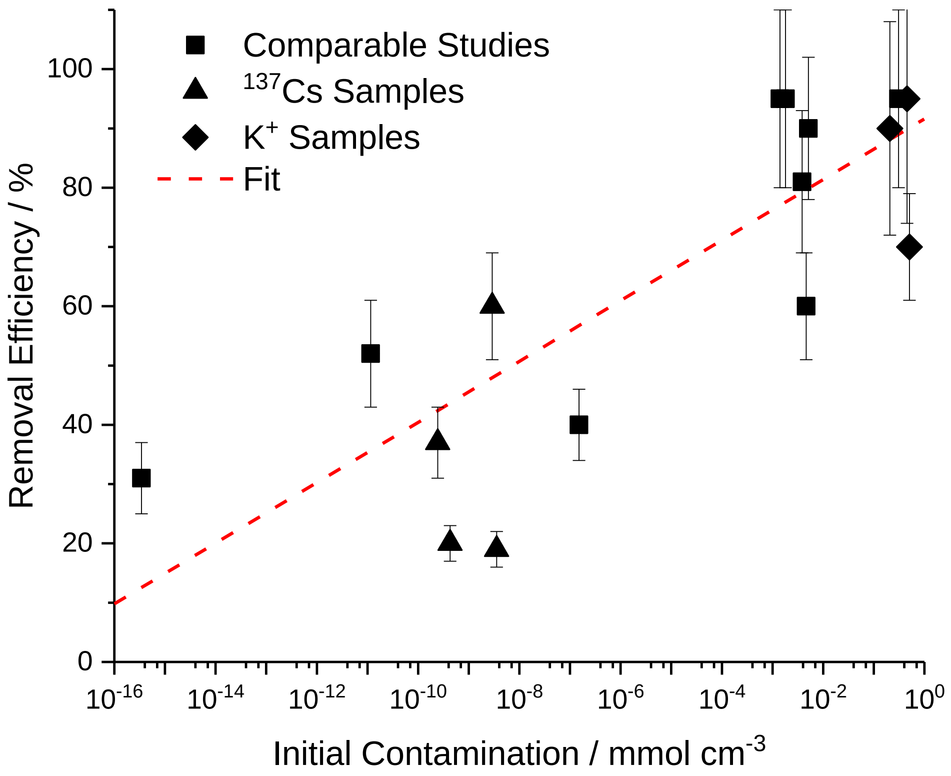

Figure 6. The relationship between the initial contamination in a concrete sample and the final removal efficiency recorded following electrokinetic decontamination, for studies broadly similar in design to the experiments carried out in this work, the red-dashed line is y = 0.0215ln(x) + 0.903, R^2 = 0.62.

This is an important result in the context of the existing literature and for the application of electrokinetics as an *in situ* decontamination. The chemicals used in the majority of literature studies for increasing electrokinetic decontamination efficiency are hazardous and their use is restricted on nuclear sites, particularly in high-dose environments. The observed effectiveness of ionic salt washing to replicate similar decontamination factors achieved with common enhancement agents provides a considerable benefit. The quantity of ionic salt need to decontaminate a large concrete sample would not pose the same safety complications as similar volumes of EDTA or HCl. This result offers a solution to one of the main obstacles to electrokinetic treatment becoming a viable concrete decontamination tool in the nuclear industry. However, with respect to hazards, Cl^- itself is a common corrosion risk in the construction industry and the mitigation of the effects are widely studied.

5. *Conclusion*

The removal of K^+ and ^{137}Cs from concrete samples was conducted adopting an electrokinetic treatment, using an applied voltage of 60V and current limit of 35mA. The levels of initial contamination ranged from 0.208-0.521mmol cm^{-3} for K^+ contaminated samples to 0.25-3.55 x 10^{-10}mmol cm^{-3} for ^{137}Cs contaminated samples. The results show that the decontamination efficiency was between 75-95% for K^+ and 19-21% for ^{137}Cs. When a 396mol m^{-3} ionic salt wash of KCl was used alongside the electrokinetic treatment the decontamination efficiency of ^{137}Cs increased threefold up to 60%, consistent with literature decontamination efficiencies for similar experimental design, shown in Table 1. We believe this is the first known description of experiments combining electrokinetic techniques and ionic salt washes to remediate radioactive concrete.

The results of this work highlights the relationship between the initial level of contamination and the achievable removal efficiencies, where at lower levels of contamination the contaminate ions are bound to strongly adsorbing sites within the concrete. In the case of this work it requires the addition of a high concentration ionic salt wash to ion exchange with a proportion of these ions, hence the increased removal efficiency of the ionic salt wash over just the electrokinetic treatment alone.

Because the decontamination efficiencies have been achieved without the use of hazardous chemicals the technique could be more easily adopted on nuclear sites, particularly in high-dose environments, where the use of powerful chemicals is restricted. Further work is being carried out to refine the treatments and develop a practical technology.

Acknowledgements

This work was funded by the UK's NDA through a PhD bursary for Andrew Parker. Colin Boxall is supported by the Lloyd's Register Foundation. Malcolm Joyce is a Royal Society Wolfson Research Merit Award holder.

References

[1] Nuclear Decommissioning Authority, The 2013 UK Radioactive Waste Inventory: Radioactive Waste Composition, (2014).

[2] Nuclear Decommissioning Authority, UK Radioactive Waste Inventory, 2014.

[3] Department of Energy & Climate Change, Strategy for the management of solid low level radioactive waste from the non-nuclear industry in the United Kingdom - Anthropogenic radionuclides, 2012.

[4] V. Kumar, R. Goel, R. Chawla, M. Silambarasan, R.K. Sharma, Chemical, biological, radiological, and nuclear decontamination: Recent trends and future perspective, J. 3 (2010) 220–238.

[5] U.S. Epa, N. Homeland, Technology Evaluation Report Decontamination of Concrete with Aged and Recent Cesium Contamination Technology Evaluation Report Decontamination of Concrete with Aged and Recent Cesium Contamination, (2013).

[6] Office for Nuclear Regulation, GDA Step 2 Assessment of the Radioactive Waste Management, Spent Fuel Management and Decommissioning Arrangements for Generic Design Assessment of Hitachi GE's UK Advanced Boiling Water Reactor (UK ABWR), 2014.

[7] K.R. Reddy, C. Cameselle, eds., Electrochemical remediation technologies for polluted soils, sediments and groundwater, John Wiley & Sons LTd, 2009.

[8] S. Barba, J. Villasenor, M.A. Rodrigo, P. Canizares, Effect of the polarity reversal frequency in the electrokinetic-biological remediation of oxyfluorfen polluted soil, Chemosphere. 177 (2017) 120–127. doi:10.1016/j.chemosphere.2017.03.002.

[9] O. Cuevas, R.A. Herrada, J.L. Corona, M.G. Olvera, S. Sep??lveda-Guzm??n, I. Sir??s, E. Bustos, Assessment of IrO2-Ta2O5|Ti electrodes for the electrokinetic treatment of hydrocarbon-contaminated soil using different electrode arrays, Electrochim. Acta. 208 (2016) 282–287. doi:10.1016/j.electacta.2016.05.045.

[10] C. Sandu, M. Popescu, E. Rosales, M. Pazos, G. Lazar, M.Á. Sanromán, Electrokinetic oxidant soil fl ushing : A solution for in situ remediation of hydrocarbons polluted soils, J. Electroanal. Chem. 799 (2017) 1–8. doi:10.1016/j.jelechem.2017.05.036.

[11] P.P. Falciglia, D. Malarbì, F.G.A. Vagliasindi, Removal of mercury from marine sediments by the combined application of a biodegradable non-ionic surfactant and complexing agent in enhanced-electrokinetic treatment, Electrochim. Acta. 222 (2016) 1569–1577. doi:10.1016/j.electacta.2016.11.142.

[12] W. Zulfiqar, M.A. Iqbal, M.K. Butt, Pb2+ ions mobility perturbation by iron particles during electrokinetic remediation of contaminated soil, Chemosphere. 169 (2017) 257–261. doi:10.1016/j.chemosphere.2016.11.083.

[13] L. Yuan, X. Xu, H. Li, Q. Wang, N. Wang, H. Yu, The influence of macroelements on energy consumption during periodic power electrokinetic remediation of heavy metals contaminated black soil, Electrochim. Acta. 235 (2017) 604–612. doi:10.1016/j.electacta.2017.03.142.

[14] A. Altaee, R. Smith, S. Mikhalovsky, The feasibility of decontamination of reduced saline sediments from copper using the electrokinetic process, J. Environ. Manage. 88 (2008) 1611–1618. doi:10.1016/j.jenvman.2007.08.008.

[15] S. Zhao, L. Fan, M. Zhou, X. Zhu, X. Li, Remediation of copper contaminated kaolin by electrokinetics coupled with permeable reactive barrier, Procedia Environ. Sci. 31 (2016) 274–279. doi:10.1016/j.proenv.2016.02.036.

[16] E. Vieira dos Santos, F. Souza, C. Saez, P. Cañizares, M.R. V Lanza, C.A. Martinez-Huitle, M.A. Rodrigo, Application of electrokinetic soil flushing to four herbicides: A comparison, Chemosphere. 153 (2016) 205–211. doi:10.1016/j.chemosphere.2016.03.047.

[17] K.R. Reddy, C.Y. Xu, S. Chinthamreddy, Assessment of electrokinetic removal of heavy metals from soils by sequential extraction analysis., J. Hazard. Mater. 84 (2001) 279–296.

[18] Y.B. Acar, R.J. Galeb, A.N. Alshawabkeh, R.E. Marks, W. Puppala, M. Brickad, R. Parkere, Electrokinetic remediation : Basics and technology status, J. Hazard. Mater. 40 (1995) 117–137.

[19] G.N. Kim, S.S. Kim, U.R. Park, J.K. Moon, Decontamination of Soil Contaminated with Cesium using Electrokinetic-electrodialytic Method, Electrochim. Acta. 181 (2015) 233–237. doi:10.1016/j.electacta.2015.03.208.

[20] G.N. Kim, B. IL Yang, W.K. Choi, K.W. Lee, Development of vertical electrokinetic-flushing decontamination technology to remove 60Co and 137Cs from a Korean nuclear facility site, Sep. Purif. Technol. 68 (2009) 222–226. doi:10.1016/j.seppur.2009.05.015.

[21] R. Lopez-Vizcaino, V. Navarro, M.J. Leon, C. Risco, M.A. Rodrigo, C. Saez, P. Canizares, Scale-up on electrokinetic remediation: Engineering and technological parameters, J. Hazard.

Mater. 315 (2016) 135–143. doi:10.1016/j.jhazmat.2016.05.012.

[22] Environmental Protection Agency, Evaluation of Five Technologies for the Mechanical Removal of Radiological Contamination from Concrete Surfaces, 2011.

[23] G. Kim, B. Yang, W. Choi, K. Lee, J. Hyeon, Washing-electrokinetic decontamination for concrete contaminated with cobalt and cesium, Nucl. Eng. Technol. 41 (2009) 1079–1086.

[24] G.-N. Kim, W.-K. Choi, K.-W. Lee, Decontamination of radioactive concrete using electrokinetic technology, J. Appl. Electrochem. 40 (2010) 1209–1216. doi:10.1007/s10800-010-0088-8.

[25] A.Y. Yurchenko, Y. V. Karlin, A.N. Nikolaev, O.K. Karlina, A.S. Barinov, Decontamination of radioactive concrete, At. Energy. 106 (2009) 225–230. doi:10.1007/s10512-009-9156-8.

[26] K.I. Popov, I. V. Glaskova, S. V. Myagkov, A.A. Petrov, Removal of cesium from the porous surface via the electrokinetic method in the presence of a chelating agent, Colloid J. 68 (2006) 743–748. doi:10.1134/S1061933X06060111.

[27] K. Popov, I. Glazkova, V. Yachmenev, A. Nikolayev, Electrokinetic remediation of concrete: effect of chelating agents., Environ. Pollut. 153 (2008) 22–28. doi:10.1016/j.envpol.2008.01.014.

[28] D.W. DePaoli, M.T. Harris, I.L. Morgan, M.R. Ally, Investigation of Electrokinetic Decontamination of Concrete, Sep. Sci. Technol. 32 (1997) 387–404.

[29] M. Castellote, C. Andrade, C. Alonso, Nondestructive decontamination of mortar and concrete by electro-kinetic methods: application to the extraction of radioactive heavy metals., Environ. Sci. Technol. 36 (2002) 2256–2261.

[30] F. Frizon, S. Lorente, C. Auzuech, Nuclear decontamination of cementitious materials by electrokinetics: An experimental study, Cem. Concr. Res. 35 (2005) 2018–2025. doi:10.1016/j.cemconres.2005.02.008.

[31] H.L. Lomasney, A.K. SenGupta, V. Yachmenev, Electrokinetic decontamination of concrete, 1996.

[32] M.Y. Miah, K. Volchek, W. Kuang, F.H. Tezel, Kinetic and equilibrium studies of cesium adsorption on ceiling tiles from aqueous solutions., J. Hazard. Mater. 183 (2010) 712–717. doi:10.1016/j.jhazmat.2010.07.084.

[33] K. Volchek, M.Y. Miah, W. Kuang, Z. DeMaleki, F.H. Tezel, Adsorption of cesium on cement mortar from aqueous solutions., J. Hazard. Mater. 194 (2011) 331–337. doi:10.1016/j.jhazmat.2011.07.111.

[34] M.D. Kaminski, S.D. Lee, M. Magnuson, Wide-area decontamination in an urban environment after radiological dispersion: A review and perspectives, J. Hazard. Mater. 305 (2016) 67–86. doi:10.1016/j.jhazmat.2015.11.014.

[35] K.R. Reddy, Electrokinetic remediation of soils at complex contaminated sites:Technology status, challenges, and opportunities, in: Coupled Phenom. Environ. Geotech., Taylor & Francis Group LLC, 2013: pp. 131–147.

[36] A.J. Parker, C. Boxall, M.J. Joyce, A radioanalytical phantom for the electrokinetic decontamination of entrained radioactivity within concrete media, J. Radioanal. Nucl. Chem. (2014).

[37] A.J. Parker, M.J. Joyce, C. Boxall, Radiometric detection of non-radioactive caesium flux using displaced naturally abundant potassium, J. Radioanal. Nucl. Chem. 307 (2016) 769–776. doi:10.1007/s10967-015-4450-5.

[38] A.J. Parker, C. Boxall, M.J. Joyce, P. Schotanus, A thalium-doped sodium iodide well counter for radioactive tracer applications with naturally-abundant 40K, Nucl. Instruments Methods Phys. Res. Sect. A Accel. Spectrometers, Detect. Assoc. Equip. 722 (2013) 5–10. doi:10.1016/j.nima.2013.04.034.

[39] E.M. McCash, Surface Chemistry, OUP Oxford, 2000.

***Novelty Statement (maximum limit:100 words)**

Caesium-137 is ubiquitous in the field of nuclear decommissioning, and arguably the most hazardous contaminant. Various techniques exist to remediate cementitious ^{137}Cs-contaminated material, but these present additional waste management challenges. Extending its use from land and soil remediation of ^{137}Cs, several studies have highlighted the potential of electrokinetic decontamination in the clean-up of radioactive concrete. The present study extends this knowledge to incorporate ionic salt washes that enhance the treatment efficiency making the technique fundamentally safer. The study also demonstrates a potential link between the mass of contamination and the effectiveness of electrokinetic remediation.

Table 1

Table 1. Experimental removal efficiency, decontamination factor, and initial concentration for literature studies closely resembling the design of this study (above dashed line) and studies with different experimental geometry or electrolyte enhancement is used (below dashed line).

Study	Contaminant	Thickness (mm)	Approximate Contamination (mmol cm^{-3})	Removal Efficiency	DF
DePaoli et al. (1995)	Cs^+	9.5	1.8×10^{-3}	95%	20
Castellote et al. (2002) 1	Cs^+	30	1.4×10^{-3}	95%	20
Castellote et al. (2002) 2	Cs^+	75	1.51×10^{-7}	40%	1.67
Frizon et al. (2005) 1	Cs^+	18	3.84×10^{-3}	81%	5
Frizon et al. (2005) 2	Cs^+	18	0.309	95%	23
Castellote et al. (2002) 3	Cs^+	-	5.11×10^{-3}	90%	10
Popov et al. (2008) 1	Cs^+	-	3.45×10^{-16}	31%	1
Popov et al. (2008) 2	$^{137}Cs^+$	-	-	85%	7
Kim et al. (2009) 1	Cs^+	-	4.61×10^{-3}	55%	2.2
Kim et al. (2009) 2	Cs^+	-	4.63×10^{-3}	99.60%	250
Kim et al. (2010) 1	$^{137}Cs^+$	-	1.16×10^{-11}	52%	2
Kim et al. (2010) 2	$^{137}Cs^+$	-	1.16×10^{-11}	99.30%	143
Castellote et al. (2011)	Cs^+	10	-	90%	10

Table 2

Sample No.	Contaminate	Thickness (mm)	Concentration of Bath (mmol cm^{-3})	Activity Sorbed (kBq)	Mass Sorbed (mmol cm^{-3})
1	K^+	20	3	0.121 (±0.009)	0.521
2		20	3	0.105 (±0.007)	0.454
3		35	3	0.206 (±0.014)	0.508
4		65	3	0.157 (±0.010)	0.208
			Activity of Bath (kBq ml^{-1})		
5	$^{137}Cs^+$	25	0.889	328.25 (±0.56)	3.551×10^{-9}
6		25	0.604	268.61 (±0.40)	2.906×10^{-9}
7		25	0.089	39.68 (±0.08)	4.293×10^{-10}
8		25	0.042	22.61 (±0.05)	2.446×10^{-10}

Table 1. Composition of the contamination baths and the mass of contamination adsorbed onto the concrete samples, for both the K^+ and ^{137}Cs samples (all ^{137}Cs samples were 25 mm thick).

Table 3

Table 1. Complete results from the electrokinetic decontamination of concrete samples contaminated with K+ and $^{137}Cs^{+}$ carried out in this study.

Sample No.	Contaminant	Thickness (mm)	Contamination (mmol cm^{-3})	Removal Efficiency	DF	Ionic Wash (mol m^{-3})
1	K^{+}	20	0.521	0.8 ± 5%	1	-
2		20	0.454	95 ± 7%	22.22	-
3		35	0.508	70 ± 3%	3.44	-
4		65	0.208	90 ± 6%	10.12	-
5	$^{137}Cs^{+}$	25	3.551×10^{-9}	19 ± 0.13%	1.24	-
6		25	2.906×10^{-9}	*60± 0.13%	2.5	400
7		25	4.293×10^{-10}	20 ± 0.47%	1.26	-
8		25	2.446×10^{-10}	*37 ± 0.59%	1.58	135

Figure 1
Click here to download high resolution image

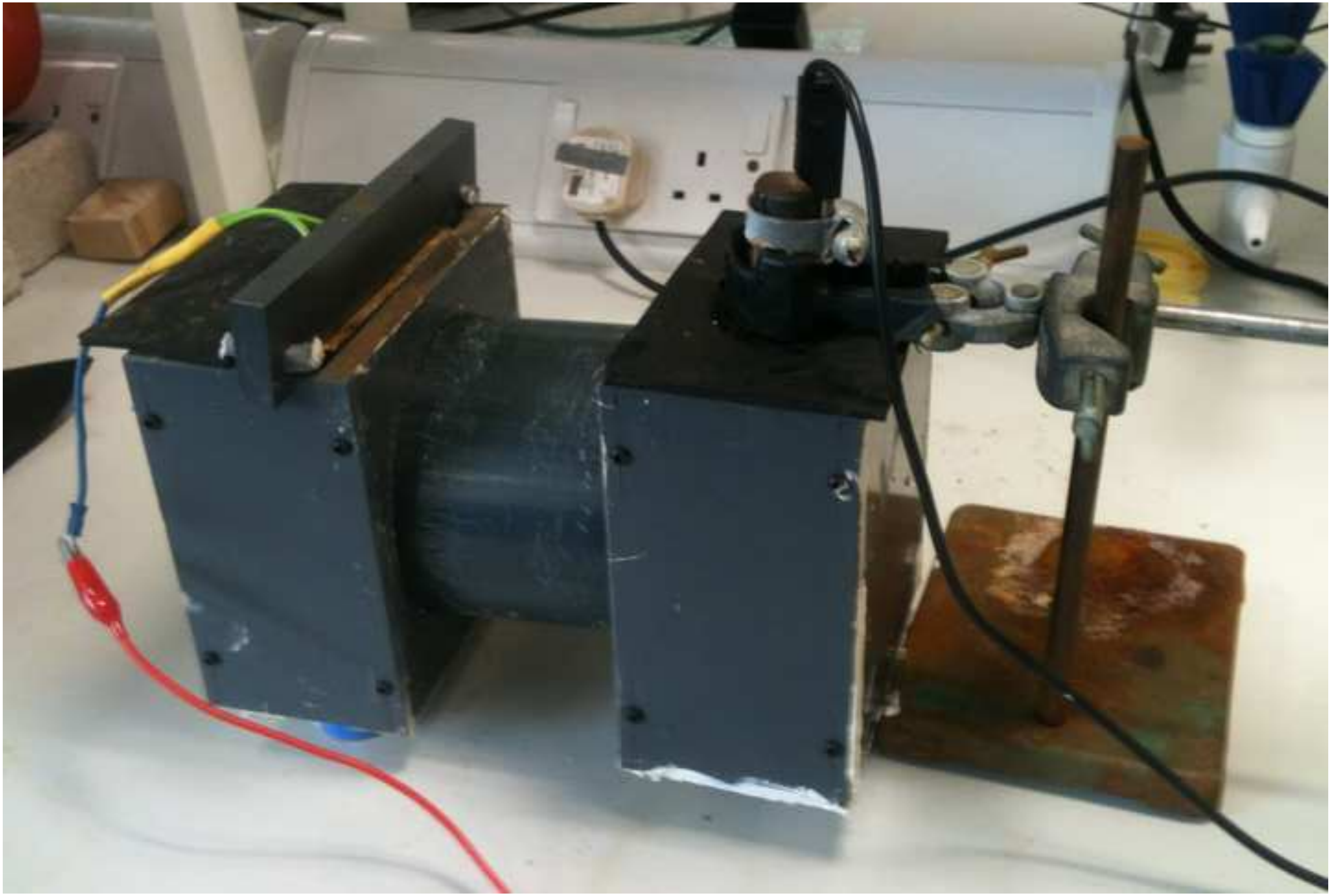

Figure 2
Click here to download high resolution image

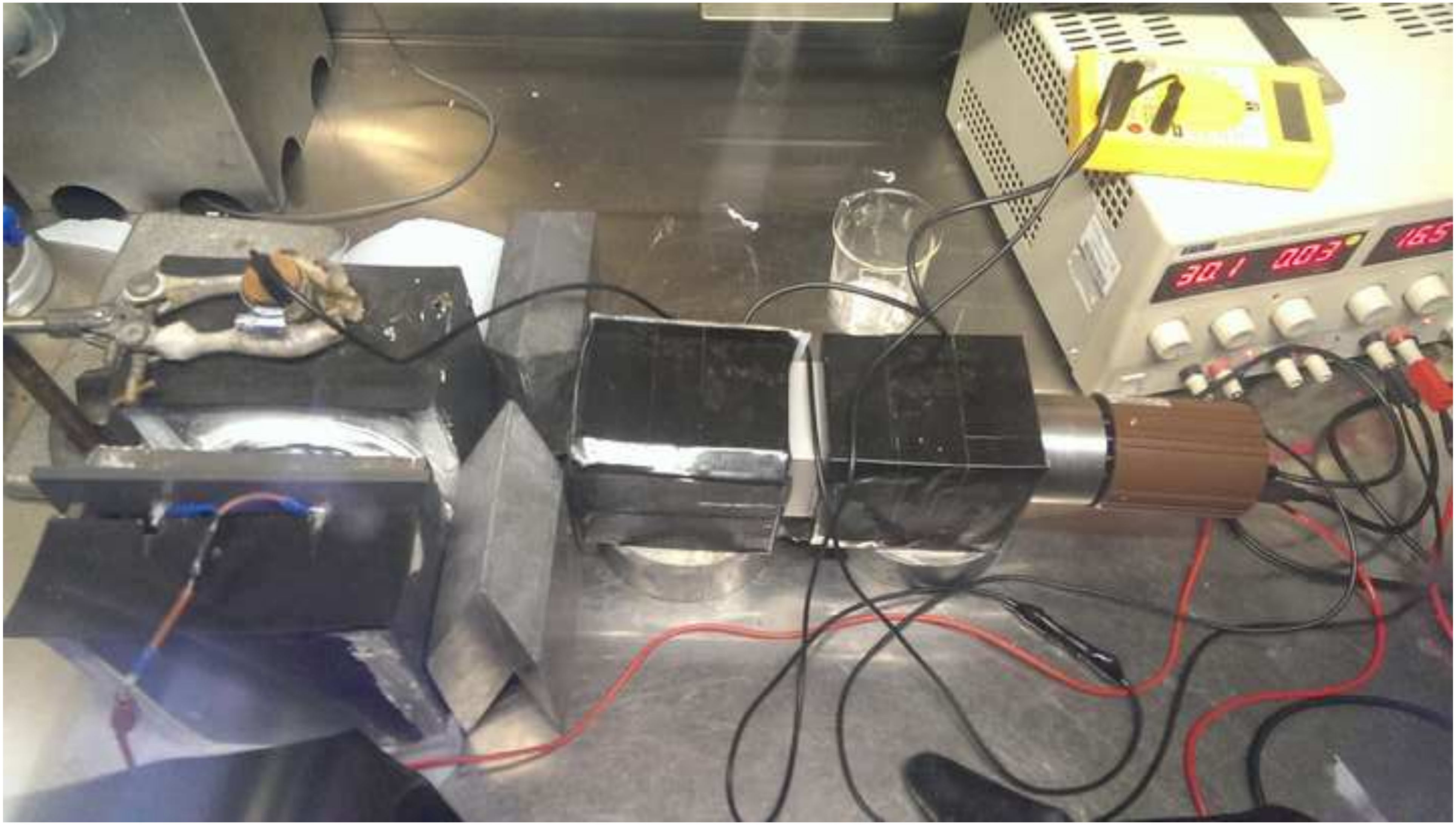

Figure 3

Click here to download Figure: Figure 4.eps

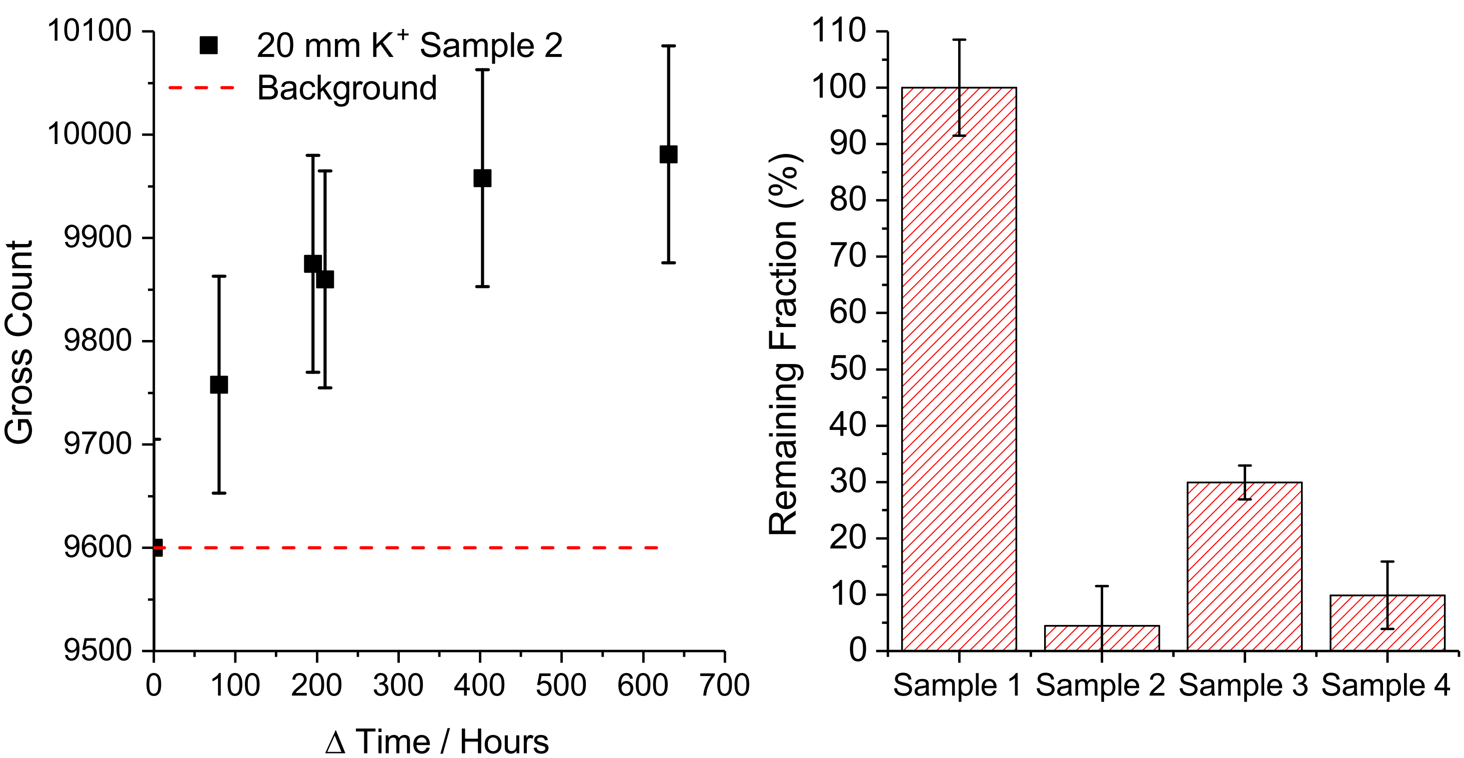

Figure 4

Click here to download Figure: Figure 5.eps

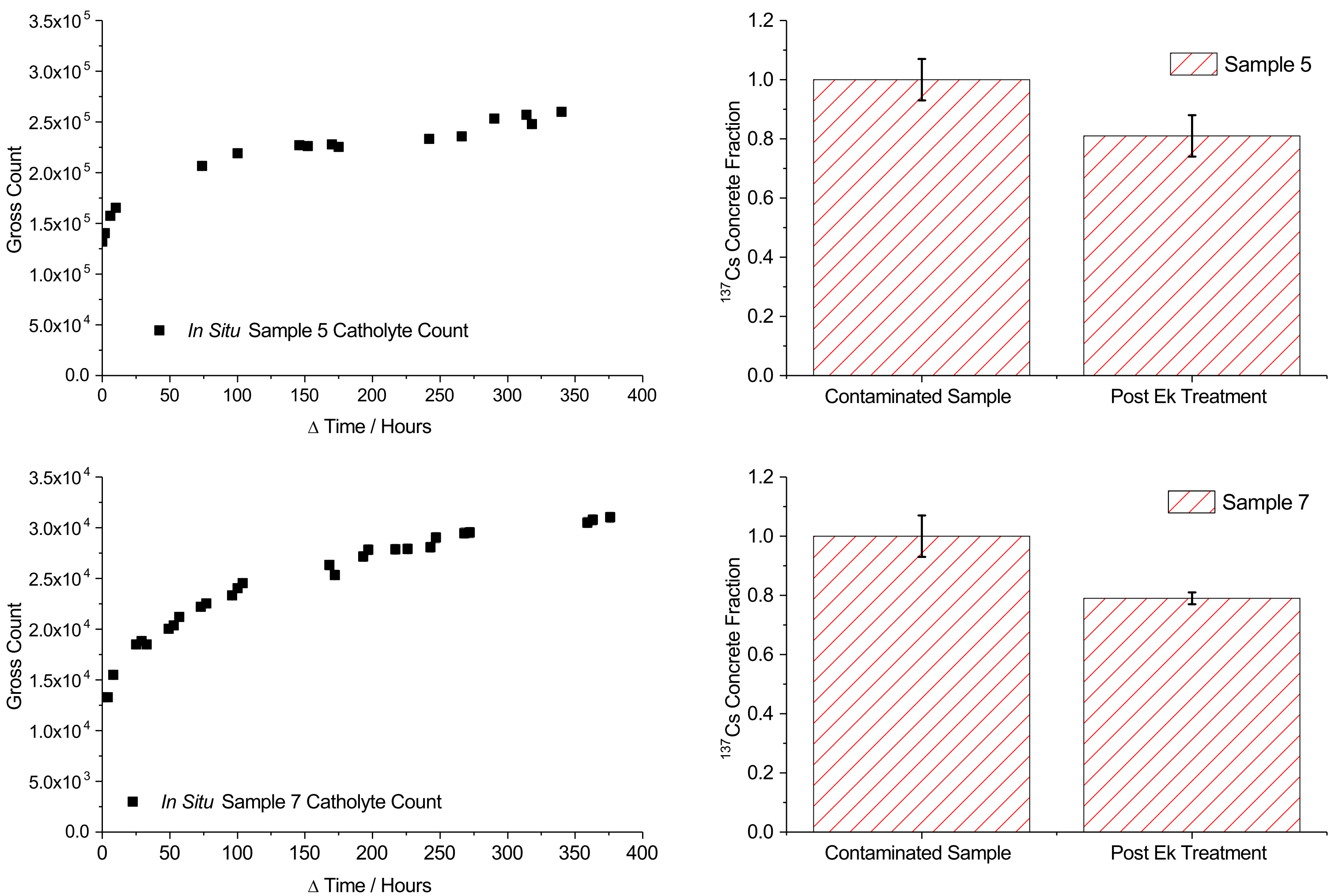

Figure 5
Click here to download Figure: Figure 6.eps

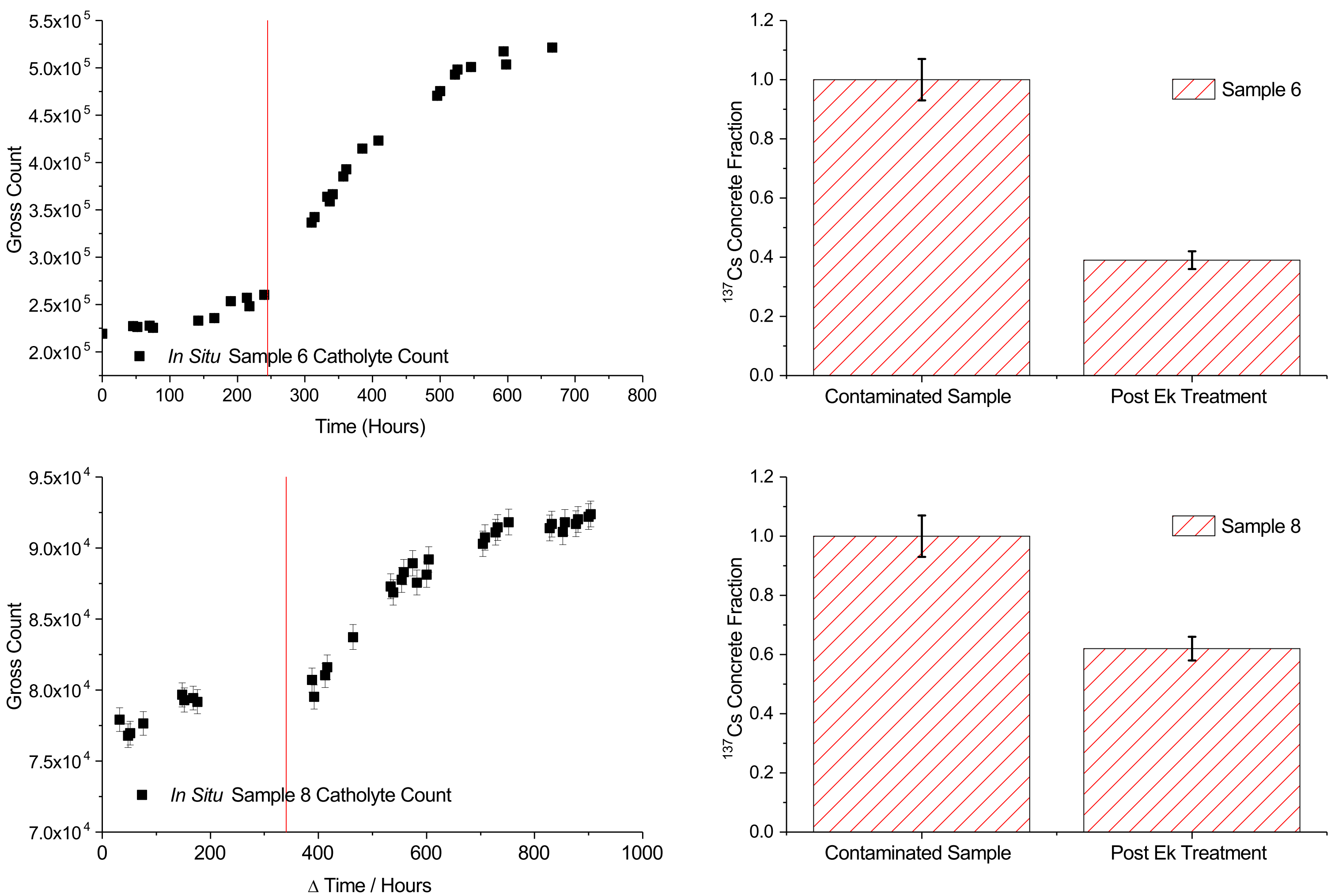

Figure 6

Click here to download Figure: Figure 7.eps